

Protective effect of fermented vegetable compounds against nonalcoholic fatty liver disease using metabolite profiling, integrated network pharmacology, and molecular docking approach

Ermin Rachmawati,
Larasati Sekar Kinasih,
Nabila Rahmadani¹,
Tias Pramesti Griana,
Roihatul Muti'ah¹, Suharti Suharti²,
Dwiki Pramudika Abdul Azis³,
Endah Eni

Departments of Biomedical Sciences and ¹Pharmacy, ³Professional Medical Doctor Program, Faculty of Medicine and Health Sciences, UIN Maulana Malik Ibrahim Malang, ²Department of Chemistry, Faculty of Mathematics and Natural Science, Universitas Negeri Malang, East Java, Indonesia

J. Adv. Pharm. Technol. Res.

ABSTRACT

Vegetable fermentation extract (VFE) shows potential as a preventive agent to inhibit nonalcoholic fatty liver disease (NAFLD). This study identified bioactive compounds of VFE and explored the mechanism of VFE against NAFLD. Metabolite profiling was analysed using Liquid chromatography-tandem mass spectrometry (LC-MS/MS). The bioactive compounds were screened using the Lipinski Rule of 5, toxicity, and biological activity prediction, followed by network pharmacology and molecular docking. Of the 24 bioactive compounds identified, 8 compounds passed the screening process. Twenty-four genes from network pharmacology were involved in the NAFLD mechanism, including those related to insulin signaling, inflammation, and lipid metabolism. Kaempferol, apigenin, and N-(p-coumaroyl) serotonin showed a good binding affinity with CCR2, AKT, IL-6, and PPAR- γ compared to simvastatin and metformin. Bioactive compounds from VFE were predicted to ameliorate NAFLD.

Key words: Metabolite profiling, molecular docking, network pharmacology, nonalcoholic fatty liver disease, vegetable fermentation

INTRODUCTION

Nonalcoholic fatty liver disease (NAFLD) has emerged as a prevalent liver disease and leads to severe complications. The development of NAFLD is closely linked to inflammation, lipid metabolism disturbance, and insulin resistance (IR).^[1-3]

Address for correspondence:

Mrs. Larasati Sekar Kinasih,
Jl. Locari, Tlekung, Junrejo, Kota Batu, Jawa Timur,
East Java 65151, Indonesia.
E-mail: larasatisekark@kedokteran.uin-malang.ac.id

Submitted: 15-Oct-2024

Revised: 28-Mar-2025

Accepted: 07-Apr-2025

Published: 19-May-2025

Access this article online

Quick Response Code:



Website:

<https://journals.lww.com/JAPTR/>

DOI:

10.4103/JAPTR.JAPTR_331_24

The consumption of fermented vegetables has been positively associated with improved health.^[4,5] While previous studies on vegetable fermentation exclusively focused on a single type of vegetable, recent findings suggested the enhancement of antioxidant capacity and the longer shelf life of vegetable fermentation by incorporating herbs, spices, and other vegetables.^[6-8] Therefore, this research explored the potential combination of cucumber and cabbage fermentation with basil leaves and chili sauces, inspired by "sambal lalapan," a traditional Indonesian side dish to inhibit NAFLD.

This is an open access journal, and articles are distributed under the terms of the Creative Commons Attribution-NonCommercial-ShareAlike 4.0 License, which allows others to remix, tweak, and build upon the work non-commercially, as long as appropriate credit is given and the new creations are licensed under the identical terms.

For reprints contact: WKHLRPMedknow_reprints@wolterskluwer.com

How to cite this article: Rachmawati E, Kinasih LS, Rahmadani N, Griana TP, Muti'ah R, Suharti S, *et al.* Protective effect of fermented vegetable compounds against nonalcoholic fatty liver disease using metabolite profiling, integrated network pharmacology, and molecular docking approach. *J Adv Pharm Technol Res* 2025;16:92-8.

Numerous studies demonstrated the spontaneous fermentation of vegetables carried out at room temperature for a week. However, in the 1st week of sauerkraut fermentation, there was an increase in nitrite production, posing potential health risks such as gastrointestinal cancer and methemoglobinemia. The decrease of nitrite and the increase of lactic acid bacteria were observed in 3–14 weeks of fermentation. Consequently, this study adopted a 21-day fermentation period, which made it novel.

Furthermore, investigating the pharmacological effects of fermented products through *in vivo* analysis requires an extensive optimization period and is expensive. Therefore, an integrative approach using metabolite profiling, network pharmacology, and molecular docking has become the solution.^[9]

MATERIALS AND METHODS

Vegetable specimen

The components of spicy sauce were onion, garlic, chili, and basil leaves. The vegetable ingredients were white cabbage, cucumber, and tomato. Every component was collected and determined at Materia Medica Batu, Indonesia.

Fermentation and extract preparation

The overnight salted cabbage was mixed with chopped cucumber, basil leaves, and sugar. The spontaneous fermentation took place for 21 days at 20°C. Extraction was performed using 70% ethanol in a 1:20 ratio (w/v) with the ultrasonic-assisted extraction technique for 30 min at room temperature.^[10]

Metabolite profiling using liquid chromatography-tandem mass spectrometry

C18 column (1.8 μ m; 2.1 mm \times 150 mm) and LC-MS/MS systems with a QToF analyzer and positive ESI ionization source were used. 100°C and 350°C were set for elution of water/formic acid (99.9/0.1 [v/v]) and acetonitrile/formic acid (99.9/0.1 [v/v]). 10 mg of the extract was dissolved in 10 ml methanol. A 5 μ L mixture was put into the device. Mass Lynx 4.1 software (Waters, Massachusetts, USA) and PubChem (<https://pubchem.ncbi.nlm.nih.gov/>) were used for chromatogram analysis. The error margin of <5 ppm was used as the final determination of the bioactive compound.

Screening of bioactive compounds

Evaluation of the potential as orally administered drugs was carried out using Lipinski's rule of 5 from <http://www.swissadme.ch/>.^[11] Assessment of the safety profile was carried out by toxicity predictions using Protox III Online Tools (<https://tox.charite.de/protox3/>). Bioactivity predictions were conducted via PASS Online (<https://www.way2drug.com/passonline/predict.php>).^[11] The compounds without no violation, toxicity level >3, and Pa >0.7 were used as cutoff for this step.

Network pharmacology

Network pharmacology analysis was conducted through the following steps: (1) Identification of genes associated with NAFLD using the DisGeNET (<https://disgenet.com/>); (2) Identification of target genes of the bioactive compounds from VFE, using the GeneCards database (<https://www.genecards.org/>); (3) Determination of overlapping genes between the disease-related genes and the compound-targeted genes using Cytoscape; (5) Protein-protein interaction (PPI) network and module analysis of

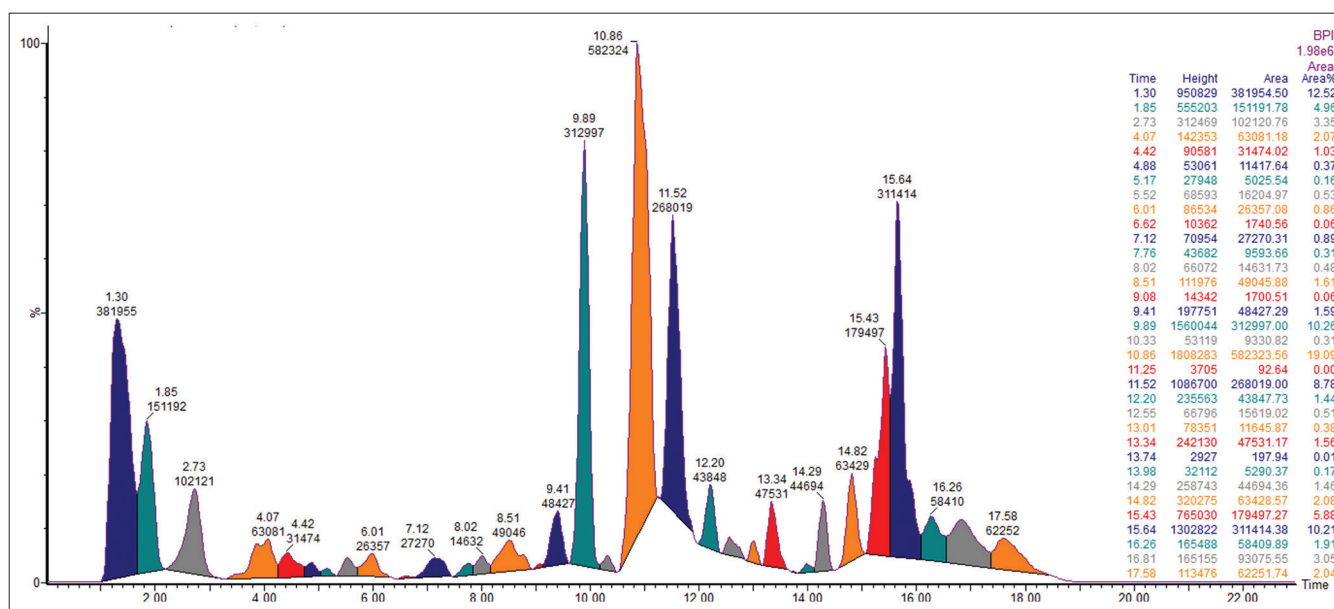


Figure 1: Chromatogram of vegetable fermentation extract

Table 1: Metabolite profiling of vegetable fermentation extract

Retention time	Area (%)	Graphical mass (m/z)	Molecular formula	Compound	Classification of compound (Chem/MesH tree)	Reference (PubChem ID, Legacy ID)
1.30	12.52	224.068	C ₁₁ H ₁₂ O ₅	Sinapinic Acid	Endogenous metabolites	ID: 1192
1.85	4.96	293.147	C ₁₂ H ₂₃ NO ₇	3-Methyl-2-[[2,3,4-trihydroxy-5-(hydroxymethyl) oxolan-2-yl] methylamino] pentanoic acid	Isoleucine derivative	CID: 139292115
2.73	3.35	328.139	C ₁₅ H ₂₁ NO ₇	N-(1-Deoxy-1-fructosyl) phenylalanine	Monosaccharide derivative	CID: 101039148
4.07	2.07	456.174	C ₂₀ H ₂₈ N ₂ O ₁₀	N-Fructosyl glutamylphenylalanine	Glycoprotein	CID: 139292055
4.42	1.03	286.047	C ₁₅ H ₁₀ O ₆	Kaempferol	Flavanol	ID: 966
4.88	0.37	209.013	C ₁₀ H ₁₆ N ₂ O ₃ S	Biotin	Monocarboxylic acid	ID: 336
5.17	0.16	166.06	C ₉ H ₁₀ O ₃	3-(4-Hydroxyphenyl)-propionic Acid	Phenolic acid	ID: 9965
5.52	0.53	464.095	C ₁₅ H ₁₄ O ₇	(-)-Epigallocatechin	Flavonoid	ID: 6131
6.01	0.86	-	-	-	-	-
6.62	0.06	213.146	C ₈ H ₁₆ N ₆ O	N-isopropyl-4-methoxy-6-(1-methylhydrazino)-1,3,5-triazin-2-amine		CID: 5215337
7.12	0.89	216.175	C ₁₅ H ₂₁ N	Pyridine, 1-butyl-1,2,3,6-tetrahydro-4-phenyl-	Cyclic compound	CID: 179808
7.76	0.31	270.052	C ₁₅ H ₁₀ O ₅	Apigenin	Flavonoid	ID: 20
8.02	0.48	-	-	-	-	-
8.51	1.61	322.131	C ₁₉ H ₁₈ N ₂ O ₃	N-(p-Coumaroyl) Serotonin	Alkaloid phenolic	ID: 6228
9.08	0.06	578.163	C ₂₇ H ₃₀ O ₁₄	Kaempferitrin	Flavonoid	ID: 6207
9.41	1.59	610.573	C ₂₇ H ₃₀ O ₁₆	Rutin	Flavonoid	ID: 28
9.89	10.26	610.573	C ₂₇ H ₃₀ O ₁₆	Rutin	Flavonoid	ID: 28
10.33	0.31	578.163	C ₂₇ H ₃₀ O ₁₄	Kaempferitrin	Flavonoid	ID: 6207
10.86	19.09	306.206	C ₁₈ H ₂₇ NO ₃	Capsaicin	Alkaloid phenolic	CID: 1548943
11.25	0.00	478.335	C ₂₀ H ₄₃ N ₇ O ₆	2-aminoethyl N-[2-[(6-amino-1-carbamoyloxyhexan-2-yl) amino]-2-oxoethyl]-N-(5-aminopentyl) carbamate; propenamide		CID: 142056458
11.52	8.78	464.095	C ₂₁ H ₂₀ O ₁₂	Quercetin-3β-D-glucoside	Flavonoid	ID: 1472
12.20	1.44	318.300	C ₁₈ H ₃₉ NO ₃	Phytosphingosine	Amino alcohol	CID: 122121
12.55	0.51	578.163	C ₂₇ H ₃₀ O ₁₄	Kaempferitrin	Flavonoid	ID: 6207
13.01	0.38	610.573	C ₂₇ H ₃₀ O ₁₆	Rutin	Flavonoid	ID: 28
13.34	1.56	610.573	C ₂₇ H ₃₀ O ₁₆	Rutin	Flavonoid	ID: 28
13.74	0.01	-	-	-	-	-
13.98	0.17	611.403	C ₃₂ H ₅₀ N ₈ O ₄	2-[3-[[2-[4-[7-(6-amino-2-butoxy-8-oxo-7H-purin-9-yl) heptyl] piperazin-1-yl] ethyl-methylamino] methyl] phenyl] acetic acid		CID: 16225952
14.29	1.46	324.290	C ₂₀ H ₃₇ NO ₂	Linoleic monoethanolamide	Fatty acids	CID: 5283446
14.82	2.08	268.264	C ₁₇ H ₃₃ NO	1-(piperidin-1-yl) dodecan-1-one	Volatile compound	CID: 246811
15.43	5.88	282.279	C ₁₈ H ₃₅ NO	Oleamide	Fatty amide	CID: 5283387
15.64	10.21	270.279	C ₁₇ H ₃₅ NO	Capsiamide	Acetamides	CID: 47346
16.26	1.91	284.295	C ₁₈ H ₃₇ NO	Stearic acid amide	Fatty amide	CID: 31292
16.81	3.05	-	-	-	-	-
17.58	2.04	-	-	-	-	-

the overlapping target genes were performed using the STRING database (version 12.0) (<https://string-db.org/>). This included enrichment analysis for KEGG pathways, WikiPathways, and Gene Ontology Biological Processes.^[12]

Molecular docking

The bioactive compounds that passed the initial screening process were selected as ligands, while simvastatin

and metformin served as control ligands.^[13] Network pharmacology analysis identified key receptors and proteins involved in NAFLD pathogenesis, including the insulin signaling pathway (IRS1, AKT), inflammation (IL6R, TNFR, CCR2), and liver metabolism (PPARγ and AdipoR1). The water molecules, the native ligands, and the heteroatom molecules in of protein were removed using Biovia Discovery Studio 2021 software.^[13]

PyRx was a Python prescription that integrated Autodock and Open Babel for molecular docking. The specific grid box and the binding site for docking are provided in Supplementary File 1. Biovia Discovery Studio 2021 software was employed to visualize the two- and three-dimensional interaction. Docking results were evaluated based on the binding affinities of -5 kcal/mol as the minimum threshold, as well as compared with the control.^[13]

RESULTS

Metabolite profiling of vegetable fermentation extract

Thirty-four compounds from LC-MS/MS are presented in Figure 1. The chromatogram analysis identified 24 compounds, as summarized in Table 1. Three compounds with the highest percentage areas were capsaicin (19.09%), sinapinic acid (12.52%), and capsiamide (10.21%).

Screening of bioactive compound

Eight compounds displayed oral drug properties, were not toxic, and had biological activities that matched with NAFLD [Table 2].

Network pharmacology

Network pharmacology determined 24 genes, 704 nodes, 885 edges, 2.514 average neighbors, 6 network diameters, 3 network radius, characteristic path length: 2.983, clustering coefficient: 0.000, network density: 0.004, network heterogeneity: 7.674, and network centralization: 0.553 [Figure 2]. Enrichment analysis from PPI network results is shown in Table 3. Data obtained from KEGG pathways, WikiPathways, and biological processes indicate involvement in inflammation, insulin resistance (IR), and lipid metabolism.

Molecular docking analysis

Based on the docking results in Table 4, only the interaction between sinapinic acid, kaempferol, 3-(4-hydroxyphenyl)-propionic acid, apigenin, and *n*-(*p*-coumaroyl) serotonin with the CCR2, IL6R, IRS, AKT, and PPAR γ receptor showed higher negative energy than control and/or a binding affinity value >-5 kcal/mol. Figure 3 presented the binding interaction between the ligand and receptor.

Table 2: Bioactive compound screening process

Compounds	Lipinski rule of 5					Toxicity		
	MW (g/mol)	Log P	HBA	HBD	PSA (Å ²)	Violation	LD50 (mg/kg)	Level
Sinapinic acid	224.21	1.31	5	2	75.99	0	1772	4
3-Methyl-2-[[2,3,4-trihydroxy-5-(hydroxymethyl) oxolan-2-yl] methylamino] pentanoic acid	293.31	-1.85	6	8	139.48	1	5000	5
Kaempferol	286.24	1.58	6	4	111.13	0	3919	5
N-(1-Deoxy-1-fructosyl) phenylalanine	327.33	-1.52	8	6	139.48	1	135	3
N-Fructosyl glutamylphenylalanine	456.44	-2.12	11	8	205.88	2	200	3
Biotin	244.31	0.59	3	3	103.73	0	4000	5
3-(4-Hydroxyphenyl)-propionic acid	166.17	1.31	3	2	57.53	0	2000	4
(-)-Epigallocatechin	306.27	0.42	7	6	130.61	1	10,000	6
Quercetin-3 β -D-glucoside	464.38	-0.48	12	8	210.51	2	5000	5
N-isopropyl-4-methoxy-6-(1-methylhydrazino)-1,3,5-triazin-2-amine	212.25	0.43	5	2	89.19	0	503	4
Pyridine, 1-butyl-1,2,3,6-tetrahydro-4-phenyl	215.33	3.52	1	0	3.24	0	150	3
Apigenin	270.24	2.11	5	3	90.90	0	2500	5
N-(<i>p</i> -Coumaroyl) Serotonin	322.36	2.57	3	4	85.35	0	500	4
Kaempferitrin	578.52	-0.42	14	8	228.97	3	5000	5
Rutin	610.52	-0.51	16	10	269.43	3	5000	5
Capsaicin	305.41	3.43	3	2	58.56	0	47	2
2-aminoethyl N-[2-[(6-amino-1-carbamoyloxyhexan-2-yl) amino]-2-oxoethyl]-N-(5-aminopentyl) carbamate; propanamide	477.60	-0.41	9	6	232.11	3	1800	4
Phytosphingosine	317.51	3.60	4	4	86.71	0	3500	5
2-[3-[[2-[4-[7-(6-amino-2-butoxy-8-oxo-7H-purin-9-yl) heptyl] piperazin-1-yl] ethyl-methylamino] methyl] phenyl] acetic acid	610.79	2.93	9	3	145.84	2	1190	4
Linoleic monoethanolamide	323.51	-	2	2	49.33	-	50,000	6
1-(piperidin-1-yl) dodecan-1-one	267.45	4.61	1	0	20.31	0	1190	4
Capsiamide	269.47	5.04	1	1	29.10	0	3200	5
Oleamide	281.48	5.29	1	1	43.09	1	750	4
Stearic acid amide	283.49	5.54	1	1	43.09	1	1000	4

MW: Molecular weight, HBA: Hydrogen bond acceptors, HBD: Hydrogen bond donors, PSA: Polar surface area

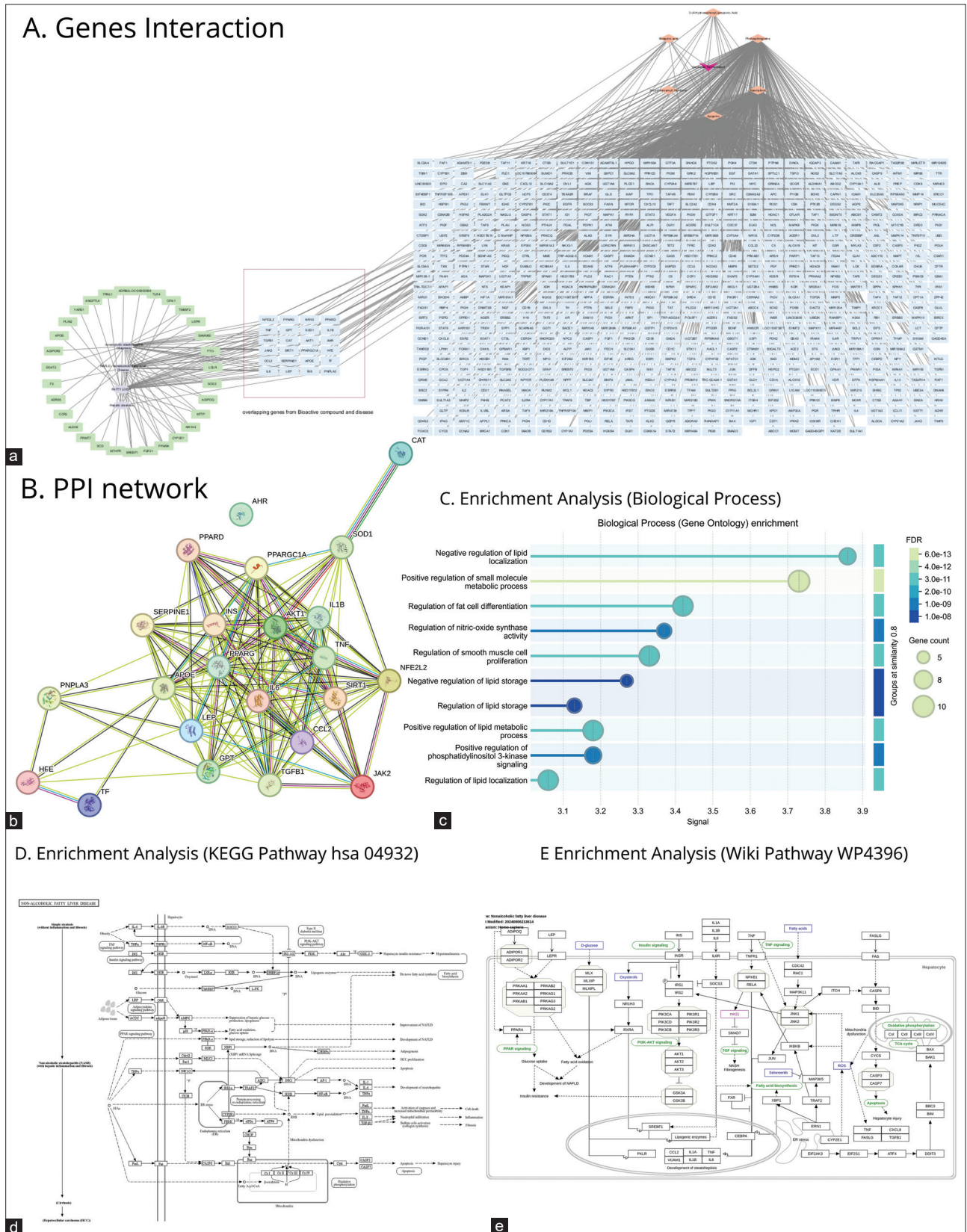


Figure 2: Network pharmacology and module analysis. (a) Gene interaction perspective. Magenta triangle; orange diamond; purple oval; green, and blue box indicated vegetable fermentation; bioactive compound; disease associated with nonalcoholic fatty liver disease (NAFLD); gene involved in disease mechanism, which is not the target of the bioactive compound; bioactive compound targets. The red line in the middle was the overlapping genes between the disease and the target of bioactive compounds. (b) Protein interaction. Nodes represent relevant targets, and edges indicate protein–protein associations. Number of nodes: 23; number of edges: 149. (c-e) Enrichment analysis linked to NAFLD

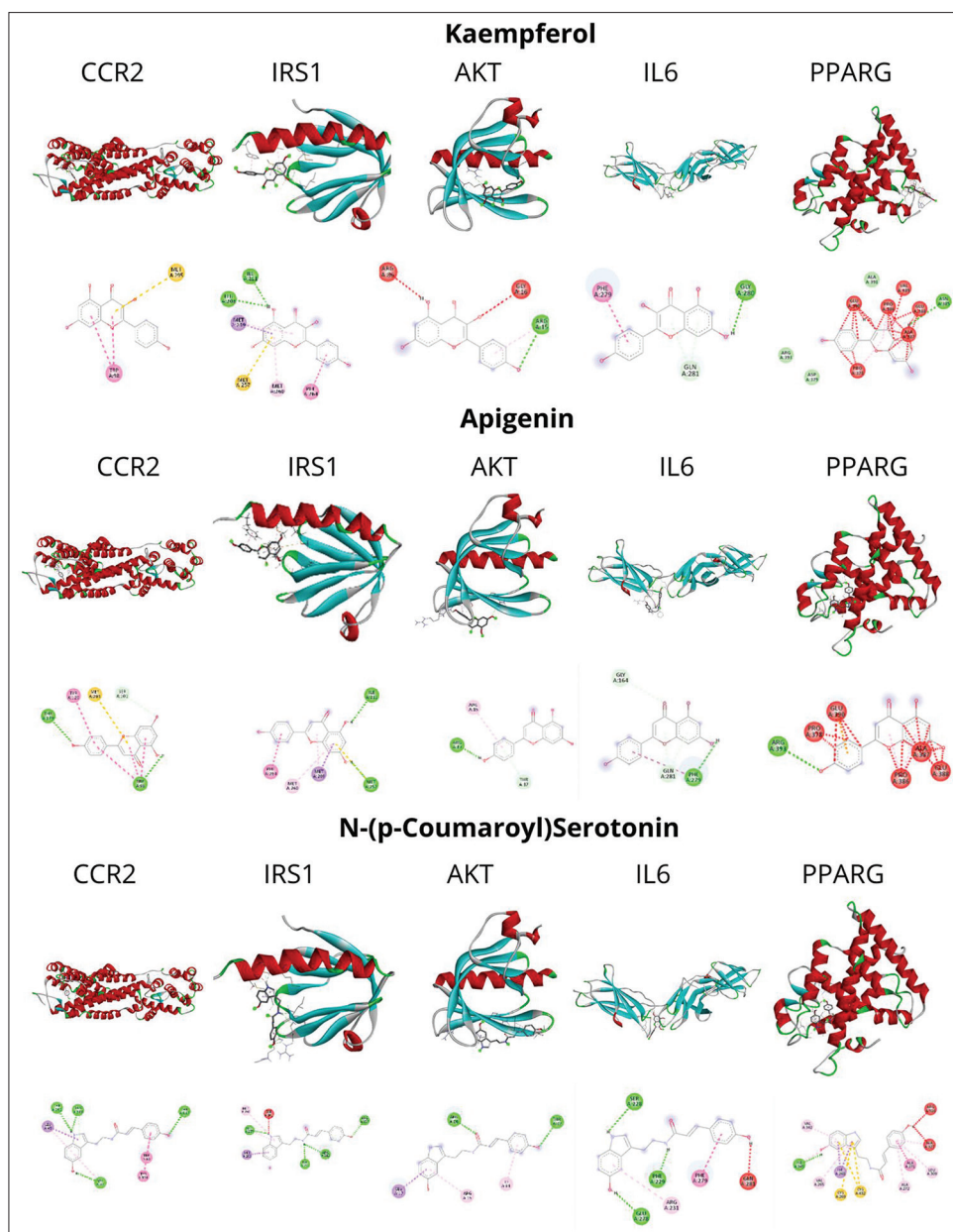


Figure 3: Two- and three-dimensional visualization of docking result

Table 3: The relevant pathways of nonalcoholic fatty liver disease matched with vegetable fermentation extract

Pathway	Description
hsa04933	Age-RAGE signaling pathway in diabetic complications
hsa04932	NAFLD
hsa04920	Adipocytokine signaling pathway
WP236	Adipogenesis
WP5113	Transcription factor regulation in adipogenesis
WP5285	NAFLD

NAFLD: Nonalcoholic fatty liver disease

DISCUSSION

The network pharmacology and docking result demonstrated

the connection between the VFE bioactive compound and the development of NAFLD. Previous experimental studies support this finding. Using several *in vitro* and *in vivo* models, sinapinic acid and apigenin have been proven to prevent cirrhosis through the suppression of inflammation and oxidative stress.^[14,15] N-p-coumaroyl serotonin, one polyphenol with antioxidant capacity, effectively inhibits α -glucosidase activity.^[16] Wang *et al.* reported that propionic acid ameliorated mitochondrial dysfunction induced by the excess of fatty acid and oxidative stress by upregulating PPAR γ coactivator 1 alpha in hepatocytes.^[17] Several studies demonstrated that kaempferol and apigenin protect against NAFLD by improving insulin sensitivity and lipid metabolism in the liver.^[18-20]

Table 4: Result of docking validation

PDB code	Ligand	Binding affinity (kcal/mol)						
		CCR2 (5T1A)	IRSI (IIRS)	AKT (2UVM)	IL6R (IN26)	TNFR (7KHD)	PPAR- γ (IFM6)	ADIPORI (5LXG)
54454	Simvastatin	-8.2	-5.8	-5.3	-5.3	-0.5	-9.4	-4.7
4091	Metformin	-4.5	-4.2	-4.3	-4.4	-3.0	-5.7	-2.9
637775	Sinapinic acid	-5.9	-4.8	-4.8	-4.3	-2.6	-5.8	-3.7
5280863	Kaempferol	-7.6	-6.3	-5.9	-5.2	2.8	-7.5	-4.9
10394	3-(4-Hydroxyphenyl)-propionic acid	-6.1	-4.3	-4.7	-3.9	-3.1	-7.2	-3.8
5280443	Apigenin	-7.9	-6.1	-5.8	-5.2	-0.4	-9.1	-4.6
5458879	N-(p-Coumaroyl) serotonin	-8.6	-6.7	-5.9	-5.4	11.4	-10.2	-5.0

Overall, the metabolite profiling of VFE and bioinformatic results conclude promising potency of VFE to be developed as a prevention strategy for NAFLD. However, the efficacy of the *in silico* method for forecasting drug efficacy in intricate biological systems may be hampered by several drawbacks due to its biological variability, the intricacy of chemical reactions, and the difficulties in precisely simulating biological systems. Therefore, future research should focus on establishing standard markers, and carrying out pharmacodynamic studies using both *in vitro* and *in vivo* methods.

CONCLUSION

Kaempferol, apigenin, and n-(p-coumaroyl) serotonin from VFE showed potential as drug-like candidates for NAFLD prevention by suppressing inflammation, IR, and increasing cholesterol storage in the liver cell.

Acknowledgment

This study was supported by DIPA FKIK UIN Malang.

Financial support and sponsorship

Nil.

Conflicts of interest

There are no conflicts of interest.

REFERENCES

- Kitade H, Chen G, Ni Y, Ota T. Nonalcoholic fatty liver disease and insulin resistance: New insights and potential new treatments. *Nutrients* 2017;9:387.
- Gruben N, Shiri-Sverdlov R, Koonen DP, Hofker MH. Nonalcoholic fatty liver disease: A main driver of insulin resistance or a dangerous liaison? *Biochim Biophys Acta* 2014;1842:2329-43.
- Fujii H, Kawada N. The role of insulin resistance and diabetes in nonalcoholic fatty liver disease. *Int J Mol Sci* 2020;21:3863.
- Yu Z, Zhang X, Li S, Li C, Li D, Yang Z. Evaluation of probiotic properties of *Lactobacillus plantarum* strains isolated from Chinese sauerkraut. *World J Microbiol Biotechnol* 2013;29:489-98.
- Asgary S, Rastqar A, Keshvari M. Functional food and cardiovascular disease prevention and treatment: A review. *J Am Coll Nutr* 2018;37:429-55.
- Patra K, Jana S, Mandal DP, Bhattacharjee S. Evaluation of the antioxidant activity of extracts and active principles of commonly consumed Indian spices. *J Environ Pathol Toxicol Oncol* 2016;35:299-315.
- Sharma L. Immunomodulatory effect and supportive role of traditional herbs, spices and nutrients in management of COVID19. *J of PeerScientist* 2020;3:1-8.
- Romano R, De Luca L, Aiello A, Pagano R, Di Pierro P, Pizzolongo F, et al. Basil (*Ocimum basilicum* L.) leaves as a source of bioactive compounds. *Foods* 2022;11:3212.
- Elkhalifa AE, Banu H, Khan MI, Ashraf SA. Integrated network pharmacology, molecular docking, molecular simulation, and *in vitro* validation revealed the bioactive components in soy-fermented food products and the underlying mechanistic pathways in lung cancer. *Nutrients* 2023;15:3949.
- Rachmawati E, Suharti S, Sargowo D, Sekar Kinasih L, Octaviano YH, Mutiah R, et al. Metabolite profiling, hypolipidemic, and anti-atherosclerosis activity of mixed vegetable fermentation extract. *Saudi Pharm J* 2023;31:639-54.
- Daina A, Michielin O, Zoete V. SwissADME: a free web tool to evaluate pharmacokinetics, drug-likeness and medicinal chemistry friendliness of small molecules. *Sci Rep* 2017;7:1-13.
- Yuan Q, Chen J, Zhao H, Zhou Y, Yang Y. Structure-aware protein-protein interaction site prediction using deep graph convolutional network. *Bioinformatics* 2021;38:125-32.
- Ferreira LG, Dos Santos RN, Oliva G, Andricopulo AD. Molecular docking and structure-based drug design strategies. *Molecules* 2015;20:13384-421.
- Jabbar AA, Alamri ZZ, Abdulla MA, AlRashdi AS, Najmaldin SK, ZainelMA. Sinapic acid attenuate liver injury by modulating antioxidant activity and inflammatory cytokines in thioacetamide-induced liver cirrhosis in rats. *Biomedicines* 2023;11:1447.
- Yue S, Xue N, Li H, Huang B, Chen Z, Wang X. Hepatoprotective effect of apigenin against liver injury via the non-canonical NF- κ B pathway *in vivo* and *in vitro*. *Inflammation* 2020;43:1634-48.
- Wang H, Fu Y, Zhao Q, Hou D, Yang X, Bai S, et al. Effect of different processing methods on the millet polyphenols and their anti-diabetic potential. *Front Nutr* 2022;9:780499.
- Wang X, Zhu M, Looor JJ, Jiang Q, Zhu Y, Li W, et al. Propionate alleviates fatty acid-induced mitochondrial dysfunction, oxidative stress, and apoptosis by upregulating PPAR γ coactivator 1 alpha in hepatocytes. *J Dairy Sci* 2022;105:4581-92.
- Li N, Yin L, Shang J, Liang M, Liu Z, Yang H, et al. Kaempferol attenuates nonalcoholic fatty liver disease in type 2 diabetic mice via the Sirt1/AMPK signaling pathway. *Biomed Pharmacother* 2023;165:115113.
- Tanase DM, Gosav EM, Costea CF, Ciocoiu M, Lacatusu CM, Maranduca MA, et al. The intricate relationship between type 2 diabetes mellitus (T2DM), insulin resistance (IR), and nonalcoholic fatty liver disease (NAFLD). *J Diabetes Res* 2020;2020:1-16.
- Tamura Y, Sugimoto M, Murayama T, Ueda Y, Kanamori H, Ono K, et al. Inhibition of CCR2 ameliorates insulin resistance and hepatic steatosis in db/db mice. *Arterioscler Thromb Vasc Biol* 2008;28:2195-201.

SUPPLEMENTARY FILE

Supplementary File 1: Definition of Catalytic Sites, Native Ligands, and Grid Boxes for Each Receptor in Molecular Docking

MOLECULAR DOCKING

The molecular docking study was conducted with the following system characteristics. Processor: AMD Ryzen 5 2500U CPU and 2.00 GHz processor, system memory: 12 GB RAM, system type: 64-bit operating system, Windows 10 as Operating System. The compounds used as ligands in the molecular docking process were selected from bioactive compounds that passed the screening as follows: sinapinic acid (PubChem CID: 637775), N-(p-coumaroyl) serotonin (PubChem CID: 458879), 3-(4-hydroxyphenyl)-propionic acid (PubChem CID: 10394), apigenin (PubChem CID: 5280443), kaempferol (PubChem CID: 5280863), and capsiamide (PubChem CID: 47346) was used as ligand control. Two-dimensional structures of the ligands from PubChem were converted to pdbqt format. The energy of the ligands was minimized using PyRx 0.9 software (Ferreira *et al.*, 2015).

Based on module analysis from previous method, several receptors and protein play an important role in NAFLD pathogenesis, including receptors in the insulin signaling pathway (IRS1 and AKT), inflammation (IL6R, TNFR, and CCR2) and liver metabolism (PPAR- γ and AdipoR1). The X-ray structure of the receptors AKT (PDB ID: 2UVM), IRS-1 (PDB ID: 1IRS), CCR (PDB ID: 5T1A), IL6R (PDB ID: 1N26), TNFR (PDB ID: 7KHD), PPAR- γ (PDB ID: 1FM6), and ADIPOR1 (PDB ID: 5LXG) was obtained from Protein Data Bank (<https://www.rcsb.org/>). The water molecules, the native ligands, and the heteroatoms molecule were removed using Biovia Discovery Studio 2021 software (Ferreira *et al.*, 2015).

IRS-1

1. Catalytic site: MET209, ARG212, ARG213, HIS216, PHE220, PHE222, ARG227, TRP237, HIS250, LEU254, MET257, MET260
2. Native ligand: 1IRS
3. Grid box:
 - Center
 - o X: -2.3607
 - o Y: -3.3576
 - o Z: -7.5346
 - Dimensions (Angstrom)
 - o X: 30.0728
 - o Y: 18.6844
 - o Z: 30.6372

AKT

1. Catalytic site: YS14, TYR18, ARG23, ARG25, ASN53, ARG86
2. Native ligand: 1IRS, 2UVM
3. Grid box:
 - Center:
 - X: 16.2784
 - Y: 6.7978
 - Z: 15.8717
 - Dimensions (Angstrom)
 - X: 19.3878
 - Y: 22.2002
 - Z: 20.8762

CCR2

1. Catalytic site: VAL37, ILE40, GLY41, LEU44, LEU45, TRP98, SER101, ALA102, THR117, TYR120, THR179, CYS190
2. Native ligand 5T1A
3. Grid box
 - Center:
 - X: 7.4351
 - Y: 27.6586
 - Z: 155.1536

- Dimensions (Angstrom)
 - X: 28.5921
 - Y: 14.6885
 - Z: 21.6600

AdipoR1

1. Binding site: GLN265, ALA268, PHE271, LEU272, LEU276
2. Native ligand: IGAG
3. Grid box
 - a. Center:
 - X: 27.6700
 - Y: 21.0487
 - Z: 11.0359
 - b. Dimensions (Angstrom)
 - X: 11.4683
 - Y: 21.0487
 - Z: 11.0359

TNFR

1. Catalytic site: ASN106, ASP109
2. Native ligand: 7KHD
3. Grid box
 - a. Center:
 - i. X: 27.858
 - ii. Y: -17.986
 - iii. Z: 51.7265
 - b. Dimensions (Angstrom):
 - i. X: 17.5126
 - ii. Y: 9.4009
 - iii. Z: 5.8191

PPAR- γ

1. Catalytic site: VAL265, ILE268, CYS269, ALA271, ALA272, GLN275, TRP305, ASN306, LEU309, ILE310, PHE313, ARG316, LEU326, ALA327, VAL342, ILE345, PHE346, VAL349, CYS432, HIS435, LEU436, PHE439, Native ligand: 7KHD
2. Native ligand: IFM6
3. Grid box:
 - a. Center:
 - i. X: 19.6467
 - ii. Y: 15.4522
 - iii. Z: 16.4814
 - b. Dimensions (Angstrom):
 - X: 22.2350
 - Y: 22.2222
 - Z: 25.4739

IL6

1. Catalytic site: PRO162, GLU163, SER228, PHE229, TYR230, ARG231, GLU278, PHE279
2. Native ligand: 1N26
3. Grid box:
 - Center:
 - o X: 7.7901
 - o Y: 56.7919
 - o Z: 94.2494
 - Dimensions (Angstrom):
 - o X: 14.6902
 - o Y: 15.7803
 - o Z: 25.0036